Biochem Genet (2018) 56:56–77
https://doi.org/10.1007/s10528-017-9829-2

ORIGINAL PAPER

DNM1L Variant Alters Baseline Mitochondrial Function and Response to Stress in a Patient with Severe Neurological Dysfunction

Kaley A. Hogarth[1] · Sheila R. Costford[2] · Grace Yoon[3] · Neal Sondheimer[2,3] · Jason T. Maynes[1,4]

Received: 26 June 2017 / Accepted: 18 October 2017 / Published online: 6 November 2017

Abstract Mitochondria play vital roles in brain development and neuronal activity, and mitochondrial dynamics (fission and fusion) maintain organelle function through the removal of damaged components. Dynamin-like protein-1 (DRP-1), encoded by *DNM1L*, is an evolutionarily conserved GTPase that mediates mitochondrial fission by surrounding the scission site in concentric ring-like structures via self-oligomerization, followed by GTPase-dependant constriction. Here, we describe the clinical characteristics and cellular phenotype of a patient with severe neurological dysfunction, possessing a homozygous *DNM1L* variant c.305C>T (p.T115M) in the GTPase domain. For comparative analysis, we also describe a previously identified heterozygous variant demonstrating a rapidly fatal

✉ Jason T. Maynes
jason.maynes@sickkids.ca

Kaley A. Hogarth
kaley.hogarth@sickkids.ca

Sheila R. Costford
sheila.cosford@sickkids.ca

Grace Yoon
grace.yoon@sickkids.ca

Neal Sondheimer
neal.sondeimer@sickkids.ca

[1] Department of Anesthesia and Pain Medicine, The Hospital for Sick Children, 555 University Avenue, Toronto M5G 1X8, Canada

[2] Division of Genetics and Genome Biology, SickKids Research Institute, 686 Bay Street, Toronto M5G 0A4, Canada

[3] Department of Paediatrics, University of Toronto, 555 University Avenue, Toronto M5G 1X8, Canada

[4] Department of Biochemistry, University of Toronto, 1 King's College Circle, Toronto M5S 1A8, Canada

neurocognitive phenotype (c.261dup/c.385:386del, p.W88M*9/E129K*6). Using patient-generated fibroblasts, we demonstrated both *DNM1L* variants undergo adverse alterations to mitochondrial structure and function, including impaired mitochondrial fission, reduced membrane potential, and lower oxidative capacity including an increased cellular level of reactive oxygen species (ROS) and dsDNA breaks. Mutation of *DNM1L* was also associated with impaired responses to oxidative stress, as treatment with hydrogen peroxide dramatically increased cellular ROS, with minimal exacerbation of already impaired mitochondrial function. Taken together, our observations indicate that homozygous p.T115M variant of *DNM1L* produces a neurological and neurodevelopmental phenotype, consistent with impaired mitochondrial architecture and function, through a diminished ability to oligomerize, which was most prevalent under oxidative stress.

Keywords *DNM1L* · DRP-1 · Mitochondrial fission · Oxidative function

Introduction

Mitochondria play a critical role in essential cellular processes, including apoptosis, calcium regulation, and energy metabolism (Westermann 2010). In contrast to their common schematic depiction as static and elliptical structures, mitochondria form extensive interconnected reticular networks that are highly dynamic. The changing shape and size of mitochondrial organelles occurs through the regulated balance between the counteracting processes of fission and fusion. Along with modulating mitochondrial morphology, these contrasting processes influence the functional state of the mitochondrial networks that ultimately dictate the energetic functional capacity of the cell (Westermann 2010). Whereas mitochondrial fission is typically associated with cell division and apoptosis, mitochondrial fusion is correlated with regeneration of mitochondrial proteins, mitochondrial DNA repair, and energy production (Hoppins et al. 2007; Knott et al. 2008; Westermann 2010). Consequently, altering the equilibrium of these opposing processes allows mitochondrial networks a mechanism to adapt to the constantly changing demands of cell.

As the cellular machinery-regulating mitochondrial dynamics have been investigated, an evolutionarily conserved group of proteins known as the dynamin-like GTPases have been identified as exerting crucial functions in both membrane fission and fusion (Schmid and Frolov 2011). One such protein, dynamin-like protein 1 (DRP-1), has been identified as a critical regulator in the mitochondrial fission process in mammals (Smirnova et al. 2001). Encoded by *DNM1L*, DRP-1 contains three domains prototypical of the dynamin-like GTPase class, with an N-terminal GTPase head, a middle domain (MD), and a C-terminal GTPase effector domain (GED), as well as a non-conserved Variable Domain (VD) (Fig. 1b) (Smirnova et al. 2001). Although the mechanism remains to be fully elucidated, cytosolically localized DRP-1 is recruited to the mitochondria through adaptor proteins, such as FIS1, in response to a variety of pro-fission physiological

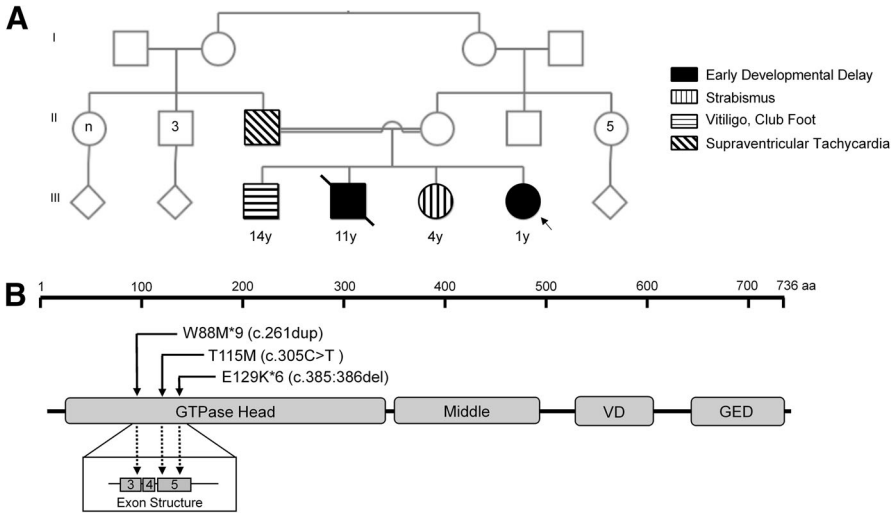

Fig. 1 *DNM1L* variant location and patient pedigree. **a** Pedigree for the p.T115M (c.305C>T) homozygote patient at time of presentation. First cousin parents produced four offspring, our patient and three siblings, with a range of pathological conditions. Proband indicated with arrow. **b** Schematic representation of DRP-1 domains with the location of patient variant indicated. The homozygous *DNM1L* mutation at c.305C>T in the patient results in a p.T115M substitution in DRP-1 in the GTPase domain. Also indicated, is the location of *DNM1L* variants from the compound heterozygote investigated for comparative analysis, which contain *DNM1L* c. 261dup/c.385:386del variants resulting in missense mutations in DRP-1 at p.W88M*9/E129K*6. Inset contains exon structure, indicating that the c.261dup (W88M*9) is located on exon 3, and both p.T115M (c.305C>T) and c.385:386del (p.E129K*6) on exon 5

cues (Clinton et al. 2016; Palmer et al. 2011). Once recruited, DRP-1 oligomerizes to form concentric ring-like structures that surround the scission site, followed by a GTPase-dependant constriction, leading to eventual fission (Smirnova et al. 2001). Along with regulating fission and fusion equilibrium in mitochondria, DRP-1 has also been demonstrated to modulate dynamics in other organelles including peroxisomes and the endoplasmic reticulum, implicating DRP-1 as a vital membrane dynamics modulator in mammalian cells (Chao et al. 2016; Schrader 2006; Yoon et al. 1998).

Mitochondria are essential organelles in most cell types, and their presence and dynamic regulation are of particular necessity to the development and function of the brain (Knott et al. 2008; Wilson et al. 2013). High energy demand and a reliance on oxidative respiration mean proper mitochondrial function is vital to neuronal health, especially for specialized functions like neurotransmitter release (Knott et al. 2008; Wilson et al. 2013). Adding further complexity is the high degree of spatial specialization and sophisticated architecture of neural cells, which requires mitochondria to be transported to (and maintained in) regions of the cell far from the nucleus (Wilson et al. 2013). As such, dysfunction of the mitochondrial fusion–fission balance has been tied to neuronal disease states. DRP-1 itself has been implicated in contributing to disease phenotypes in both sporadic and inherited neurodegenerative diseases including Alzheimer's, Parkinson's, and Charcot–Marie–Tooth Type 2A (Reddy et al. 2011). Furthermore, patients identified as

possessing a *DNM1L* variant all illustrate some degree of neurocognitive dysfunction through a mitochondrial mechanism, though the symptoms range significantly in type and severity (Chao et al. 2016; Fahrner et al. 2016; Nasca et al. 2016; Sheffer et al. 2016; Vanstone et al. 2015; Waterham et al. 2007; Yoon et al. 2016). Of these individuals, majority of these patients contain *DNM1L* mutations located in the MD, which has been proposed to result in the impaired protein oligomerics (Chao et al. 2016; Fahrner et al. 2016; Sheffer et al. 2016; Vanstone et al. 2015; Waterham et al. 2007). While mutations in the GTPase domain have been described, the mechanism by which they precipitate into dysfunctional mitochondria is not well understood (Nasca et al. 2016; Yoon et al. 2016).

Despite the relationship between DRP-1, mitochondrial dynamics and human disease, little is known regarding the cellular phenotype of patients with *DNM1L* variants. To date, there are a limited number of case reports describing patients with *DNM1L* defects, and fewer still with characterizations of the functional cellular consequences. Here, we describe a patient with the homozygous *DNM1L* variant c.305C>T (p.T115M/T115M) (Uniprot O00429-6 numbering, DRP-1 isoform 6), corresponding to the GTPase head domain of DRP-1, exhibiting significant developmental delay and neurological impairment. To our knowledge, this variant represents the first homozygous *DNM1L* variant in the literature, as well as one of only three described variants of the GTPase head domain (Nasca et al. 2016; Yoon et al. 2016). We report the clinical features and the cellular phenotype, using a previously described compound heterozygous patient (c.261dup/c.385:386del, p.W88M*9/E129K*6) for comparative analysis (Yoon et al. 2016).

Materials and Methods

Sequencing

Panel sequencing was performed on a HiSeq1500, revealing a homozygous c.305C>T (p.T115M/T115M) genome variant (ClinVar NM_012062.4, SNP rs201929226) (Medical Neurogenetics, Atlanta, GA, using their proprietary capture methodology). The presence of the variant was confirmed with Sanger sequencing, and each parent was determined to be heterozygous for the same genome alteration (reference genome GRCh37/hg19, UCSC Genome). The sequencing of the c.261dup/c.385:386del (p.W88M*9/E129K*6) (ClinVar NM_001278464.1 and SNP rs879255686/ClinVar NM_012062.4 and SNP rs879255687) patient was previously reported (Yoon et al. 2016).

Fibroblast Generation and Culture

A skin biopsy was performed for clinical testing of mitochondrial electron transport complexes. Consent was obtained for re-analysis of this sample for research-based testing using a protocol approved by the Research Ethics Board at SickKids Hospital. The wild-type samples were obtained from discarded foreskin fibroblasts after approval from the Research Ethics Board. The cells were cultured with

Dulbecco's modified eagle medium (DMEM) supplemented with 10% v/v fetal bovine serum, 1% v/v penicillin/streptomycin, and 0.5% v/v uridine (200 μM) (Sigma) at 37 °C and 5% CO_2.

Oxidative Stress Treatments

Fibroblasts were washed twice in PBS prior to treatment, followed by 2-h incubation with 20 or 200 μM H_2O_2 in phenol red free DMEM. Cells were harvested by trypsinization and washed twice with PBS prior to use in downstream applications.

Oxidative Stress, γ-H2AX, and MitoPotential Assay

We performed the Muse™ Oxidative Stress, γ-H2AX, and MitoPotential kits to measure levels of reactive oxygen species, γ-H2AX, and mitochondrial membrane potential (EMD Millipore). Assays were performed as per the manufacturer's instructions and samples were analyzed using Muse™ Cell Analyzer (EMD Millipore). Data were extracted using FlowPy software (http://flowpy.wikidot.com).

Mitochondrial Quantification qPCR

Total genomic DNA was isolated using Geneaid Tissue Genomic DNA Mini Kit as per the manufacturer's instructions. qPCR analysis performed using C100 Touch Thermal Cycler-CFX96 Real-Time PCR (Bio-Rad) as described previously, using the following primers (5′–3′): ACGCCATAAAACTCTTCACCAAAG (ND1 forward), TAGTAGAAGAGCGATGGTGAGAGCTA (ND1 reverse), TGCACCACCAACTGCTTAGC (GAPDH forward), and GGCATGGACTGTGGTCATGAG (GAPDH reverse) using Sso Fast™ EvaGreen® Supermix and performed according to the manufacturer's specifications (Santos et al. 2002). C_q values determined using CFX Manager Software (Bio-Rad, Version 3.1).

Confocal Microscopy and Image Analysis

For all staining procedures, fibroblasts were grown on black 96-Well Microplate (Greiner Bio-One) and imaged using Olympus IX81 with 60× oil-objective and 40× water-objective lenses and captured using C900-13 EM-CCD (Hamamatsu Photonics) with Volocity Software (Perkin-Elmer). For mitochondrial imaging, cells were stained with MitoTracker Green (Life Technologies) and Hoecht 33342 (Life Technologies) at 1:5000 and 1:10,000 dilutions, respectively, in media for 45 min at 37 °C (protected from light). For peroxisomal visualization, fibroblasts were fixed in 4% paraformaldehyde in PBS for 15 min at room temperature. Following fixation, cells were incubated in PMP70 primary antibody (Abcam ab3421) at 1:500 dilution, overnight at 4 °C. Following primary antibody incubation, cells were incubated in species matched AlexaFlur680 secondary antibody (1:5000) and Hoecht 33342 (Life Technologies) at 1:5000 for 45 min at 37 °C (protected from the light). Confocal images were processed in ImageJ using TopHat Filtering

algorithm (Fast Filters) before standard and default particle analysis (National Institutes of Health, https://imagej.nih.gov). For mitochondrial morphology assessment, a minimum of 450 mitochondrial fragments were analyzed over triplicate experiments.

Scratch Assay

Fibroblasts seeded at 5×10^5 cells/mL in an Ibidi Culture-Insert on a 24-well plate and grown overnight to confluence. Insert was removed, and the created cell-free gap was imaged at 0, 12, 24, and 48 h using Zeiss Axiovert 200 M on 10x objective and captured using Zeiss AxioCam CCD camera. Gap closure was quantified using ImageJ Wound Healing Tool (National Institutes of Health, https://imagej.nih.gov).

Western Blot

Using SDS-PAGE 20% (w/v), 40 µg of whole cell protein was separated and transferred to 0.2-µm-PVDF membrane with the Bio-Rad Trans-Blot Turbo Transfer System®. Membrane was blocked for 1 h, followed by overnight incubation with primary antibody for DRP-1 and GAPDH. Membrane was incubated with species-specific horseradish peroxidase-linked secondary antibody for 1 h. Protein levels were detected by Enhanced Chemiluminescence System (GE Healthcare) scanned on the Bio-Rad Gel-Doc™ XRSystem (Bio-Rad). Optical densities were obtained using ImageJ (National Institutes of Health, https://imagej.nih.gov). Antibodies used are listed as follows: monoclonal DRP-1 Pierce™ Thermo Scientific (1:500) (cat. PA1-16987) (Rockford, IL, USA), monoclonal GAPDH Sigma Life Sciences (1:3000) (cat. G8795) (St. Louis, MO, USA).

RT-qPCR

To investigate total transcriptional levels of DRP-1 isoforms, we performed RT-qPCR analysis. Total RNA was isolated from fibroblasts using Geneaid RNA isolation kit and reverse transcription (RT) completed using Maxima First Strand Synthesis Kit (Thermo Scientific), completed as per the manufacturer's instruction. Following RT, cDNA underwent qPCR with the following primers to amplify transcript variants of *DMN1L* (5′–3′): CTGCCTCAAATCGTCGTAGTG (DRP-1 forward), GAGGTCTCCGGGTGACAATTC (DRP-1 reverse), ACATCAAGAAGGTGGTGAAG (GAPDH forward), and CTGTTGCTGTAGCCAAATTC (GAPDH reverse) using Sso Fast™ EvaGreen® Supermix and performed according to the manufacturer's specifications. These primers span exon 3, allowing for determination of both total transcript and transcript containing exon 3 levels. qPCR was performed using C100 Touch Thermal Cycler-CFX96 Real Time PCR (Bio-Rad) and C_q values were determined using CFX Manager Software (Bio-Rad, Version 3.1).

Agarose DNA Gel

Following qPCR, 3 μg of PCR products were resolved on an 2% agarose gel containing 1/20,000 SafeView^{TM} Classic (ABM Inc) in 1× TAE buffer at 120 V. Gel was imaged using the Bio-Rad Gel-Doc^{TM} XRSystem using UV light (Bio-Rad) with fragment size determined using 100 bp DNA ladder (GeneDirex).

Seahorse Analysis/Oxygen Consumption Rate

To investigate the oxygen consumption rate (OCR), we performed a Seahorse XF Cell Mito Stress Test (MST) (Agilent Technologies). Cells were seeded at 20,000 per well in a 96-well plate in media containing 5.6 mM glucose. Fibroblasts OCRs were measured at baseline and in response to 1 μM oligomycin (OLA), 1.5 μM carbonyl cyanide-*4*-(trifluoromethoxy)phenylhydrazone (FCCP), and a mixture of 0.5 μM rotenone (RO) and 0.5 μM antimycin (AMA). OCR was normalized to protein content, as measured by BCA (bicinchoninic acid) assay. Data are expressed over time and were analyzed using a two-way ANOVA with Tukey post-test.

Statistical Analysis

Unless otherwise specified, results are represented as mean ± SEM of ≥ 3 independent experiments. Statistical significance was determined using paired Student's t test with p value < 0.05 considered to be a significant difference.

Results

Clinical Presentation of a Patient with *DNM1L* Variant

An infant girl was presented to our genetics clinic with a history of profound hypotonia, developmental delay, and abnormal movement. Her parents are first cousins and she was the product of an uncomplicated full term pregnancy, experiencing no medical complications during the perinatal period (Fig. 1a). Her hypotonia was noted in the first months of life. Her development peaked before one year of age, when she could track visually, hold her head up unsupported, and possessed a mature pincer grasp. She never achieved the ability to sit independently. At presentation, there were concerns about loss of existing motor milestones. Labs at her initial evaluation including lactate, plasma amino acids, and acylcarnitine were unremarkable. MRI showed bilateral symmetrical restriction of diffusion in deep gray structures. Panel sequencing identified a homozygous *DNM1L* variant at ch12:32861094 C>T (ClinVar NM_012062.4, SNP rs201929226) resulting in p.T115M mutation, located in the GTPase domain of DRP-1 (Fig. 1b), with an allele frequency of 0.000331 and 0.0002 according to ExAC and 1000 Genomes databases, respectively. The variant was predicted to be pathologic using PolyPhen (score of 1.0, "Probably Damaging") (PolyPhen v2.2), Mutation Assessor (score of 2.765, "medium functional impact"), and Mutation Taster (Prediction "disease

causing," PhyloP 5.681 and Phastcons 1, very high conservation) (Adzhubei et al. 2010; Martelotto et al. 2014). The presence of the variant in the patient was confirmed with Sanger sequencing, and similarly each parent was determined to be heterozygous for the alteration.

Gradually, the patient lost remaining developmental milestones. During the course of care, it was noted that lactate levels became intermittently elevated (up to 9.9 mM) during acute episodes of physiological stress (infections or periods where she is anorexic). Although *DNM1L* mutations can be associated with peroxisomal dysfunction, the patient had normal very long chain fatty acid (VLCFA) testing (C24:C22 ratio of 0.834 and C26:C22 ratio of 0.003, both within normal limits) which is consistent with confocal imaging, demonstrating no significant impact on peroxisomal morphology (Sheffer et al. 2016). At her most recent evaluation at 4 years of age, she was flaccid and minimally interactive to painful stimulus or to contact with her caregivers.

For comparative analysis in biochemical analysis, we also present a compound heterozygous variant of *DNM1L* (c.261dup/c.385:386del, p.W88M*9/E129K*6) occurring in the GTPase head domain of DRP-1 (Fig. 1b) (Uniprot O00429-6 numbering, DRP-1 isoform 6) which we previously identified in two siblings (Yoon et al. 2016). Parental testing confirmed that the mutations were present in trans. The two patients were born to non-consanguineous parents and delivered by caesarean section at 36–37 weeks due to fetal distress, with physical exams revealing reduced birth weight, head circumference, and body length. The siblings were similarly born with profound hypotonia, absent respiratory effort, and lacked deep tendon reflexes and spontaneous movements. Both patients died following withdrawal of ventilatory support before 1 month of age. For comparative analysis to the newly identified p.T115M/T115M variant, we examined fibroblasts from one of the two siblings.

DRP-1 Protein Levels

To determine the impact of the *DNM1L* variant on protein expression in the patient fibroblasts, we performed Western blots on whole cell lysate (Fig. 2). We observed two distinct bands at approximately 75 and 280 kDa in all fibroblasts (including WT), corresponding to monomeric and oligomeric forms of DRP-1, respectively (Zhao et al. 2011). As has been previously observed with DRP-1, oligomers can be observed under reducing conditions with SDS-PAGE (Qi et al. 2013). These oligomers represent homotetramers, consistent with the mechanism of DRP-1 association on the mitochondrial membrane (Koirala et al. 2013). Both variants showed increased levels of monomeric DRP-1 (approximately 3- and 2-fold for the p.T115M/T115M and p.W88M*9/E129K*6 variants, respectively) and a lower abundance of oligomerized DRP-1 (approximately 2- and 4-fold reduction for the p.T115M/T115M and p.W88M*9/E129K*6 variants, respectively), compared to the WT fibroblasts (Fig. 2). This relationship implies that the *DNM1L* variants impair the ability of DRP-1 to undergo functionally appropriate oligomerization.

Interestingly, the cells derived from the p.W88M*9/E129K*6 patient still express monomeric DRP-1, despite possessing a non-sense variant in each *DNM1L* allele. The two mutations reside in different exons of *DNM1L*, with the c.261dup allele

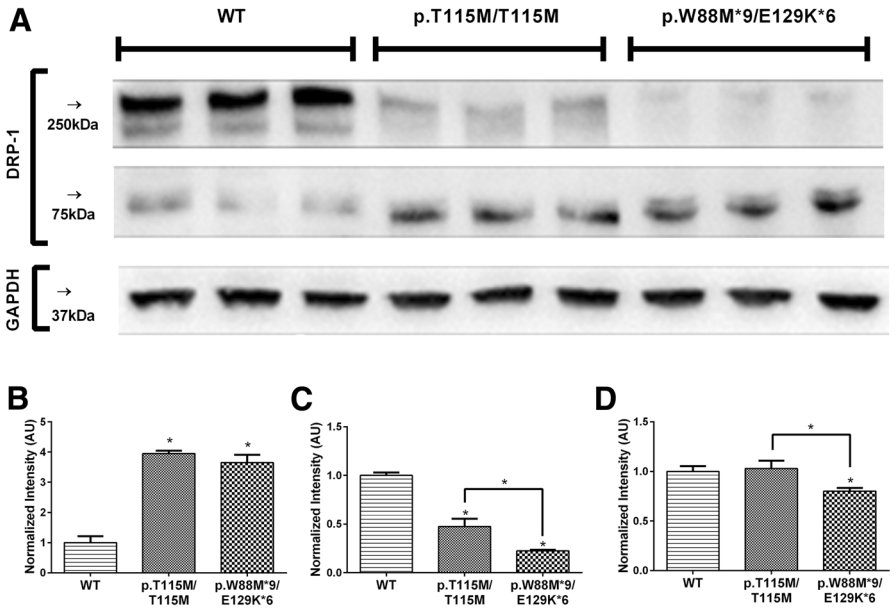

Fig. 2 Immunoblotting analysis of DRP-1. **a** Immunoblot of whole cell lysates isolated from DRP-1 variants and wild-type (WT) fibroblasts probed with α-DRP-1. Quantification of 75 kDa (**b**), 250 kDa (**c**), and total protein (**d**) bands, with DRP-1 levels normalized to GAPDH and represented in arbitrary units (AU). *DNM1L* variants simultaneously demonstrated a significant increase of monomeric, and significant decrease in oligomeric DRP-1 compared to WT cells. Values represent means with error bars representing ± SEM. Statistical significance was determined by Student's *t* test, with p value < 0.05 indicated with (*)

(p.W88M*9) contained in exon 3, and the c.385:386del allele (p.E129K*6) contained in exon 5 (Fig. 1b). Six of eight described DRP-1 splice isoforms do not contain exon 3, but Ou et al. has demonstrated that inclusion of exon 3 may contribute to neural-specific DRP-1 functions (in particular splice isoform 6, Uniprot ID O00429-6) (Strack et al. 2013; Uo et al. 2009). Exon 3 only encodes for 14 amino acids, resulting in an undetectable change in the size of the monomeric protein on SDS-PAGE (Fig. 2) (Uo et al. 2009). To determine if the protein expressed in p.W88M*9/E129K*6 cells results from a bias towards splice isoforms that remove exon 3, we analyzed RT-PCR products generated using *DNM1L* primers that span this region of the mRNA (Fig. 3). We found that the p.W88M*9/E129K*6 cells contained ~ 70% of the total *DNM1L* transcript levels compared to WT cells, consistent with our observed reduction in total protein levels (Fig. 2) and with previous observations where only a single allele of *DNM1L* was expressed (Manczak et al. 2012; Wakabayashi et al. 2009). Additionally, the transcripts in the p.W88M*9/E129K*6 cells were approximately 42 bp shorter across the exon 3 region, supporting the idea that the DRP-1 protein expressed in the p.W88M*9/E129K*6 fibroblasts likely represents a splice isoform that lacks exon 3 and bypasses the non-sense mutation in one *DNM1L* allele. No spice isoform exists that would remove the second non-sense mutation in exon 5 (c.385:386del/p.E129K*6),

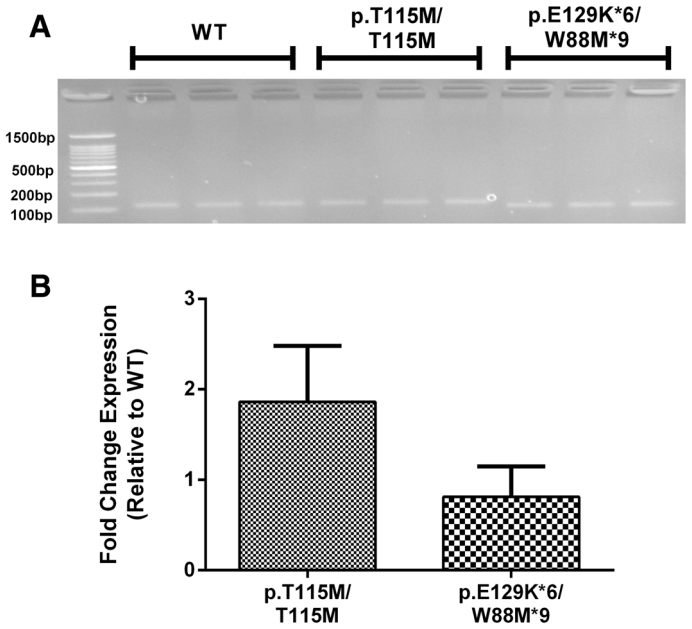

Fig. 3 Analysis of *DNM1L* transcripts. **a** Reverse transcription-qPCR (RT-qPCR) performed on total RNA isolated from mutant fibroblasts. The wild-type and p.T115M/T115M variant cells create a PCR product expected for transcripts that include exon 3 (171 bp), where the p.E129K*6/W88M*9 variant produces a PCR product 42 bp shorter, indicating the absence of exon 3. **b** Relative to wild-type (WT) fibroblasts, the *DNM1L* variants demonstrated altered transcript expression profiles. Error bars represent ± SD

making it likely that the p.W88M*9/E129K*6 mutant only produces DRP-1 from a single allele.

Mitochondrial Morphology and Mass

Confocal imaging with MitoTracker Green was performed to visualize the morphological consequences of the DRP-1 variants on the mitochondria. As can be seen in Fig. 4, both variants contain elongated mitochondria with notably less branch points, as well as lack the uniform size and distribution network seen in the WT fibroblasts ($p < 0.05$ for both the average size and perimeter of mitochondrial fragments, Fig. 4g, h). This morphological defect has been observed in multiple patient-derived cells, containing a range of unique *DNM1L* variants (Chao et al. 2016; Fahrner et al. 2016; Nasca et al. 2016; Sheffer et al. 2016; Vanstone et al. 2015; Waterham et al. 2007; Yoon et al. 2016). Along with modulating morphology, mitochondrial dynamics is an important mechanism for maintaining mitochondrial DNA (mtDNA) distribution and integrity within the organelle (Lee and Wei 2005). With this in mind, we investigated mtDNA content using qPCR, which demonstrated that both p.T115M/T115M and p.W88M*9/E129K*6 fibroblasts had significantly reduced mtDNA (60 and 30% reductions, respectively), compared to

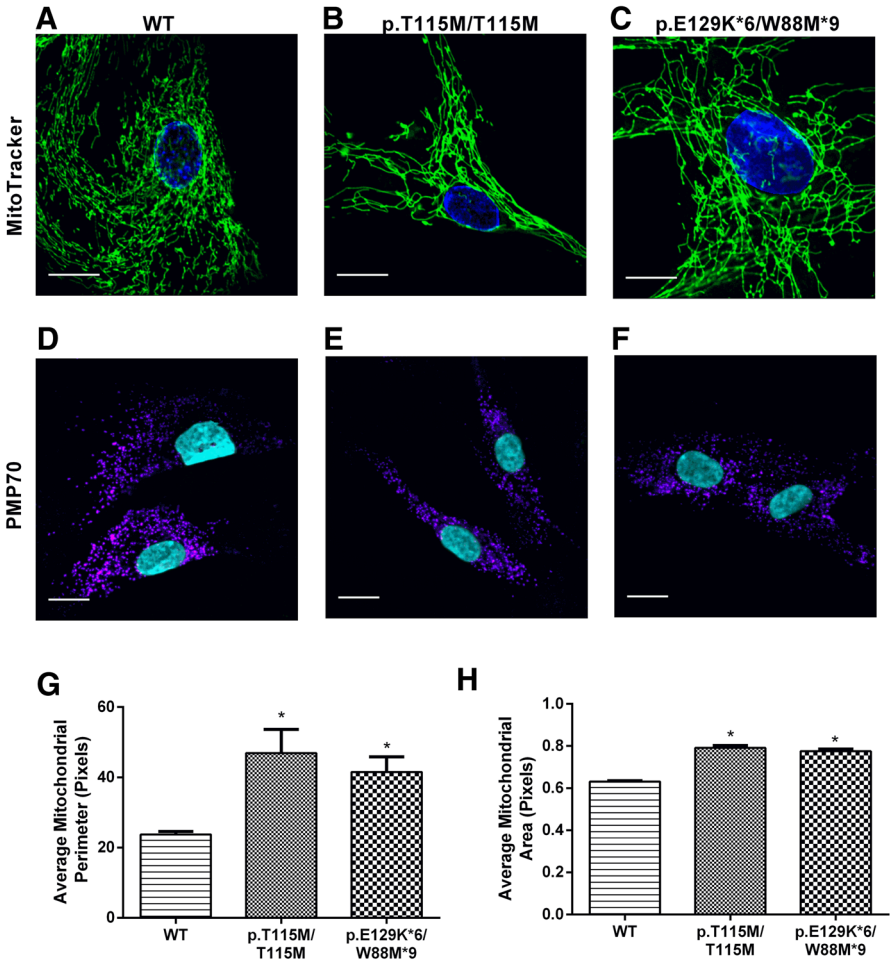

Fig. 4 Confocal microscopy analysis of patient-derived fibroblasts. **a**, **d** Wild type (WT). **b**, **e** p.T115M/T115M. **c**, **f** p.W88M*9/E129K*6. *DNM1L* variants demonstrated a deviation from the uniform and even mitochondrial distribution seen in the WT fibroblasts, including a loss of reticular pattern and longer (increased average perimeter) and larger (increased average area) mitochondrial fragments (**g**, **h**), consistent with a defect in DRP-1 activity. Peroxisomal imaging demonstrated no significant alterations to peroxisomal morphology, size, or shape in the *DNM1L* mutants, consistent with the normal values of serum VLCFA seen in the patients. Fibroblast mitochondria, peroxisomes, and nuclei were visualized with MitoTracker Green, PMP70, and Hoechst, respectively. Scale bars represent 20 mm (**a**–**c**) and 50 mm (**d**–**f**). Values represent means with error bars representing ± SEM. Statistical significance was determined by Student's *t* test, with p value < 0.05 indicated with (*)

WT fibroblasts (Fig. 4b). This reduction is consistent with previous animal investigations with *DNM1L* mutations or knockouts, which have demonstrated an association between DRP-1 level, and cellular mitochondrial content/biomass (Ishihara et al. 2009). Consistent with the normal VLCFA levels in these patients, there was no difference in peroxisomal structure when observed with PMP70 staining (Fig. 4d–f).

Mitochondrial Function at Baseline

To investigate the role of the *DNM1L* variants on mitochondrial energetic function, we performed a Seahorse XF Cell Mito Stress Test (Fig. 5a). The *DNM1L* variant fibroblast samples had significantly reduced oxygen consumption rates (OCR) compared to the WT cells ($\sim$ 60 and $\sim$ 30% OCR for the p.T115M/T115M and p.W88M*9/E129K*6, respectively), both at baseline and when respiration was uncoupled using FCCP to measure maximal capacity. This indicates that the *DNM1L* variants impair baseline respiration but also profoundly reduce the spare oxidative capacity of the cell (difference between the maximal and baseline OCR). Interestingly, the addition of oligomycin (OLA in Fig. 5a, a mitochondrial complex V inhibitor), did not alter the OCR of either of the variant fibroblast, showing that in these cells the OCR at baseline is mostly from proton leak and not from ATP production. The addition of rotenone and antimycin A (complex I and III inhibitors) brought down the OCR's in the WT and p.T115M/T115M cells to the same level, indicating that non-mitochondrial respiration is equivalent. However, the p.W88M*9/E129K*6 cells showed a lower OCR after FCCP addition (uncoupling agent), showing that severe loss of DRP-1 function may alter mitochondrial and non-mitochondrial respiration. Our findings are consistent with previous investigations that demonstrated a reduced oxygen consumption in patients with *DNM1L* substitution mutations and in cell lines with siRNA knockdown of DRP-1 in HeLa

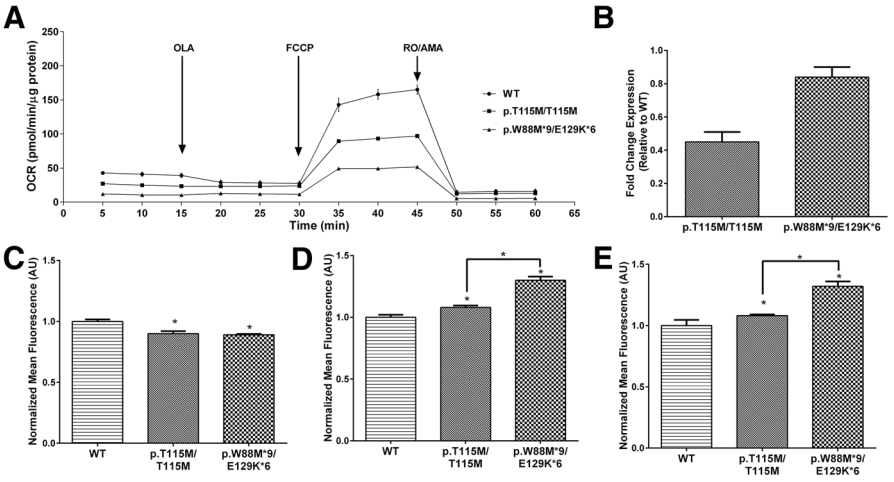

Fig. 5 Functional characterization of *DNM1L* variants. Variants consistently demonstrated a reduced functional capacity relative to the wild-type (WT) fibroblasts, with the p.T115M/T115M variant presenting an intermediate phenotype. **a** Oxygen consumption rate (OCR) (energetic capacity) was lower at baseline (pre-oligomycin A (OLA) addition) and at maximal capacity (after addition of carbonyl cyanide-*4*-(trifluoromethoxy)phenylhydrazone (FCCP)) for both variants. Antimycin A (AMA) and rotenone (RO) added to inhibit mitochondrial respiration. Relative to wild-type control, both DRP-1 variants had lower mitochondrial content (determined by qPCR) (**b**) and mitochondrial membrane potential (**c**) but higher cellular reactive oxygen species (**d**) and evidence of double-stranded DNA breaks (**e**). Values represent means with error bars representing $\pm$ SEM. Statistical significance was determined by Student's *t* test, with p value < 0.05 indicated with (*)

(Benard et al. 2007), yeast (Nasca et al. 2016), and patient isolated cells (Sheffer et al. 2016).

Consistent with a lower OCR, both *DNM1L* variants demonstrated a mild reduction in $\Delta\Psi_m$ compared to WT fibroblasts (10% reduction in both variants) (Fig. 5c). This measurement of membrane potential was the only metric where the p.T115M/T115M variant did not represent an intermediate phenotype between normal (WT) and severe (p.W88M*9/E129K*6). In previous studies with *DNM1L* variants, no change was observed in $\Delta\Psi_m$, indicating that DRP-1 impairment does not affect membrane potential or, more likely, that there is a balance between dysfunctional depolarization of the membrane and hyperpolarization as a stress response (similar to stress-induced mitochondrial hyperfusion, SIMH) (Sheffer et al. 2016; Vanstone et al. 2015). The effect of dysfunctional mitochondria was more apparent in the cellular ROS level, which was increased by 10 and 20% in the p.T115M/T115M and p.W88M*9/E129K*6 variants (Fig. 5d). As a potential consequence of increased cellular ROS, we measured the level of γ-H2AX (indicator of dsDNA breaks), which showed increases of 10 and 30% in the variant cells (Fig. 5e).

As a separate functional endpoint, we measured the ability of the patient-derived cells to grow and divide (scratch assay). As is demonstrated in Fig. 6, both variants showed a significant decrease in area coverage compared to the WT fibroblasts, with 1.5- and 4-fold reductions at all time points. Our result is similar to those described in Wakabayashi et al., who observed impaired growth in *DNM1L* variant cell lines, and is consistent with the suggestion that DRP-1-dependant mitochondrial fragmentation is required for proper mitotic division (Strack et al. 2013; Taguchi et al. 2007).

Mitochondrial Function Following Oxidative Stress (H_2O_2 Treatment)

Mitochondria contribute to the cellular response to oxidative stress through the induction of apoptosis and initiating ROS scavenging pathways (Lee and Wei 2005). We measured the functional consequences of treating the *DNM1L* variants with 20 and 200 μM H_2O_2, corresponding to mild and severe in vivo ROS (Fig. 7). A normal response to oxidative stress (similar to what we observed in our WT fibroblasts) is a loss of mitochondrial membrane potential, co-incident with damage to mitochondrial components and a reduction in respiratory function (WT cells showed reductions of 7 and 13% in $\Delta\Psi_m$ with exposure to 20 and 200 μM peroxide). However, both patient-derived lines showed altered responses, with only mild reductions (or in one case an increase) in membrane potential. The cellular ROS level was more significantly affected, in particular at 200 μM, where the two variant samples had a profound increase compared to WT control cells. Interestingly, double-stranded DNA breaks did not follow the same trend, with the *DNM1L* variant cells showing a generally smaller increase in γ-H2AX with peroxide exposure. These results suggest that the *DNM1L* mutations result in an altered capacity to respond to cellular oxidative stress.

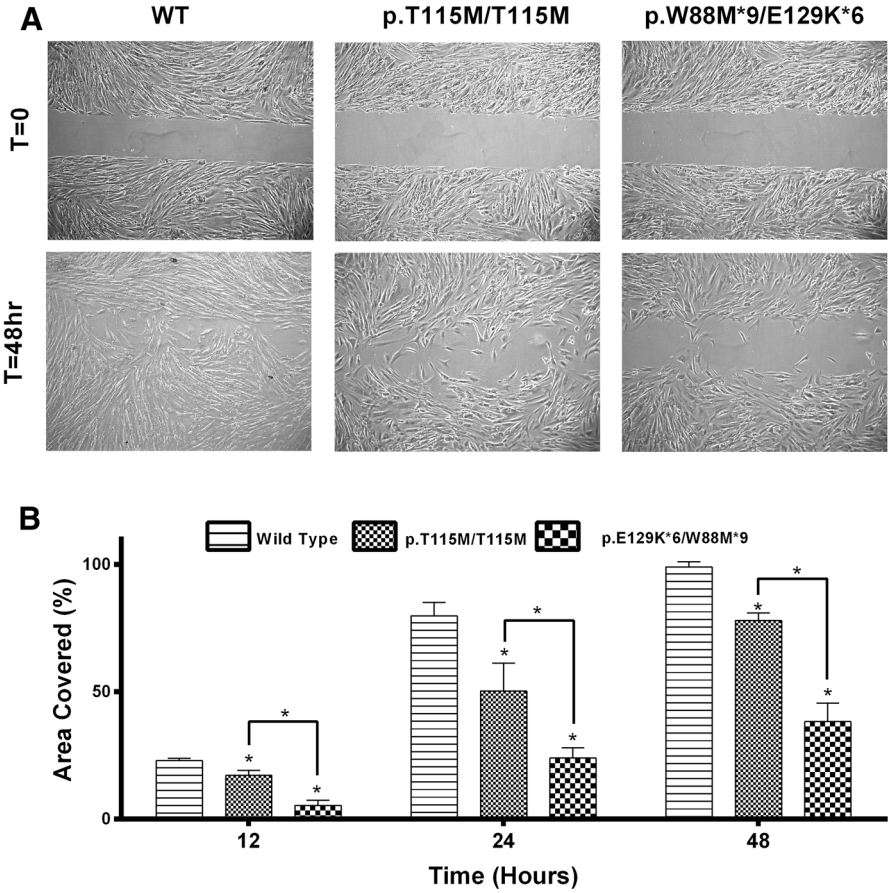

Fig. 6 Characterization of functional motility of *DNM1L* variants. *DNM1L* variants illustrated a decreased functional motility in patient-derived fibroblasts compared to wild type (WT). **a** Brightfield images of patient-derived fibroblasts after standardized scratch-assay, and **b** quantification of gap closure. Values represent means with error bars representing ± SEM. Statistical significance was determined by Student's *t* test, with p value < 0.05 indicated with (*)

DRP-1 Molecular Modeling

The mutated Thr115 residue lies at the interface where the GTPase head domains of DRP-1 converge during functional oligomerization (Fig. 8) (Jendrach et al. 2008). While monomeric in the cytosol, DRP-1 uses multiple sites of interaction in the head and tail domains to form dimers, which then oligomerize to provide functionality. The oligomers arrange around the mitochondrial membrane to facilitate membrane scission. The GTPase head provides significant interactions to stabilize the oligomers, and facilitates membrane scission through GTP hydrolysis. Thr115 does not form any direct interactions with adjoining GTPase head domains or have obvious effects on GTP hydrolysis (the nucleotide binding site is on the distal side of the head domain from Thr115). However, mutation of a threonine to a

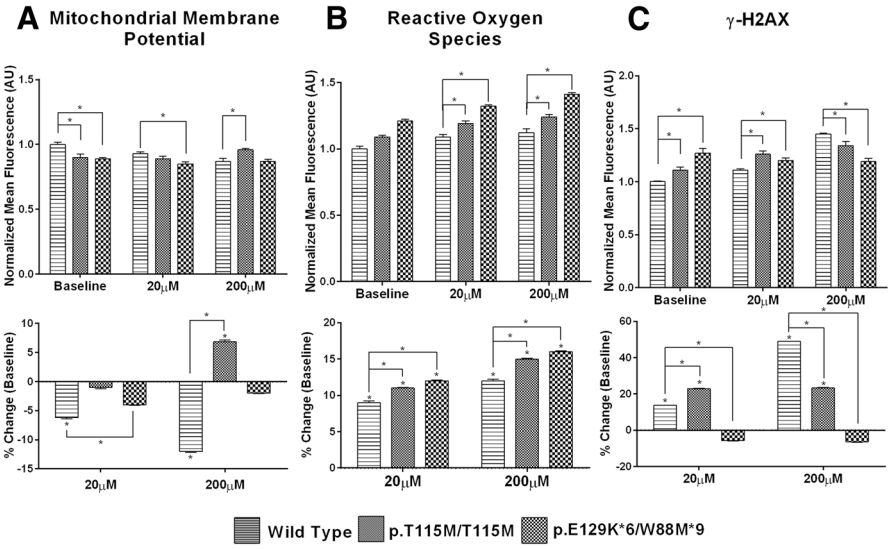

Fig. 7 Functional response of *DNM1L* variants to oxidative stress. Fibroblasts underwent mild (20 μM H_2O_2) and severe (200 μM H_2O_2) oxidative stress treatment for 2 h. Both *DNM1L* variants exhibited unique responses to oxidative stress distinct from wild type (WT). Oxidative stress induced a smaller change in mitochondrial membrane potential ($\Delta\Psi_m$) (**a**) but created a larger cellular oxidative load (ROS) (**b**) in *DNM1L* variants with both low and high oxidative stress treatment. At high oxidative load, both *DNM1L* variants induced a smaller increase in double-stranded DNA breaks (γ-H2AX) (**c**), compared to WT. Values represent means with error bars representing ± SEM. Statistical significance was determined by Student's *t* test, with p value < 0.05 indicated with (*)

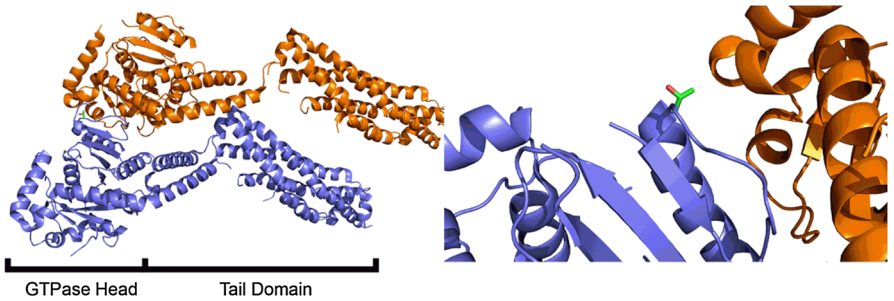

Fig. 8 Structural consequences of *DNM1L* mutation. The DRP-1 structure consists of two main regions, the GTPase head and tail domains and oligomerization occurs through contacts in both areas (a smaller third domain, the GTPase effector domain, GED, is made of the C-terminal end of the protein and lies adjacent to the GTPase head) (left). Thr115 lies at the interface of the GTPase head domains in the DRP-1 dimer, and mutation to a methionine would impede (but likely not eliminate) the ability of DRP-1 to oligomerize through steric clashes (right). The two monomers of the dimer are colored slate and orange, Thr115 is shown as green sticks (Color figure online)

methionine would introduce significant steric clashes between adjacent head domains and adversely affect DRP-1 oligomerization. The mutation would likely not abolish oligomerization, relying on the other sites DRP-1 interaction, but would

impede enzyme functionality and produce the intermediate phenotype for mitochondrial scission that we observed.

Discussion

DNM1L Influences Neurological Development

The clinical presentation of our patient, possessing a homozygous p.T115M mutation of the GTPase head domain, is similar to that described for patients with other *DNM1L* mutations. Most patients, including ours, experience symptoms consistent with neurological dysfunction, including hypotonia, abnormal brain structure, and developmental delay. These symptoms emulate observations in animal models that have shown embryonic lethality with DRP-1 abolition and severe brain hypoplasia with brain-specific knockouts (and early death), signifying a developmental role for DRP-1 in the nervous system (Ishihara et al. 2009; Wakabayashi et al. 2009). Although neurological dysfunction is common in patients with *DNM1L* variants, symptoms can vary significantly in severity, highlighting the importance of variant type and location in determining clinical phenotype. The range in clinical severity may occur as a result of residual DRP-1 function, or if the variant can be fully/partially attenuated by splice isoforms (as we observed with the p.E129K*6/W88M*9 mutation). Interestingly, our patient progressed to one year of age, acquiring developmental milestones, but her development stagnated and eventually regressed. This variable capacity to develop after birth supports a functional role of *DNM1L* in infant neurological development, distinct from its function in utero.

p.T115M/T115M Variant Affects DRP-1 Oligomerization

DRP-1 is a cytosolic protein that is recruited to the mitochondria in response to various cellular signals, which are regulated through a combination of complex post-translational modifications and differential splice isoform expression (Chang and Blackstone 2010; Dickey and Strack 2011; Strack et al. 2013). Structural studies, both EM and X-ray crystallographic, show that DRP-1 does not physically make contact with the mitochondrial membrane, and the location of most splice isoforms is in the tail domain, showing that tissue- and context-specific isoform expression may regulate which adapter proteins DRP-1 interacts with on the mitochondrial membrane to facilitate scission. While in the cytosol, DRP-1 exists primarily as a monomer, although exogenously purified protein will spontaneously oligomerize in solution, indicating that a stimulus, like phosphorylation, likely allows for DRP-1 monomer association in the crowded intracellular environment (Mears et al. 2011; Taguchi et al. 2007). Our novel variant, p.T115M/T115M, is not a known phosphorylation site, nor does it appear to have any role in the catalytic function of DRP-1. The mutated threonine residue lies beside Y101, a putative Rak kinase site (involved in cell cycle transitions), but there is no experimental evidence of Y101 phosphorylation. Our data indicate that the p.T115M/T115M variant

impairs DRP-1 oligomerization, without reducing total protein levels, and modeling shows that p.T115M/T115M may disrupt GTPase head associations (Figs. 2, 8). These findings insinuate that the functional consequences observed in our patients are due to impaired monomer association, and not defects in catalytic (GTPase) function or response to stimuli (phosphorylation). This region is the target for MiD59 inhibitory regulation of DRP-1 oligomer assembly and structural studies demonstrate that interactions between GTPase domains on adjacent helical strands enhance oligomer stability, supporting our findings (Clinton et al. 2016; Mears et al. 2011; Palmer et al. 2011). Qi et al. have demonstrated that cellular treatment with a DRP-1 GTPase inhibitor reduces oligomerization, particularly under stress conditions (Qi et al. 2013). This further supports the idea that DRP-1 may have distinct functions at baseline and during cell stress. The findings in the p.T115M/T115M variant partially contrast with the complex heterozygote p.W88M*9/E129K*6, where oligomerization is impaired, but total protein levels are also decreased, and an alternative splice isoform (which removes the W88M*9 stop codon) is expressed. In this case, a lower amount of oligomerized DRP-1 could be due to the splice isoform itself (an isoform that is less favorable to oligomerization), or just from a lower level of total protein (less protein to oligomerize). Since there are multiple sites of DRP-1 interaction in the oligomer, the p.T115M/T115M variant would likely impede, but not block association, explaining the intermediate cellular (and patient) phenotype.

Impaired DRP-1 Function Results in Reduced Metabolism and Oxidative Stress at Baseline

The p.T115M/T115M and p.W88M*9/E129K*6 cell lines had altered mitochondrial architecture, impaired growth, increased ROS and γ-H2AX levels, as well as decreased $\Delta\Psi_m$ and mtDNA content, all representative of cellular distress and mitochondrial dysfunction. These findings show that both samples have less mitochondrial mass per cell, and that the mitochondria that remain are less functional (double hit), likely resulting from the inability to remove/repair damaged mitochondrial components. At baseline, both samples have reduced oxidative metabolism (OCR), which increases cellular ROS. Mitochondria represent the primary source of ROS (as much as 90%), and damage to the organelles can lead to substantial ROS increases, most typically from electron acceptor-derived electrons reacting with molecular oxygen (Balaban et al. 2005). An elevated level of γ-H2AX in the patient-derived may result from the elevated ROS, or may be indicative of a global disruption of normal cellular processes (i.e., a failure to repair existing DNA lesions, rather than an increase in dsDNA breaks). Support for the latter includes the observation that additional oxidative stress (peroxide) was unable to significantly increase the γ-H2AX in the patient samples, and that DRP-1 is known to bind to p53 (Guo et al. 2014). Additionally, Ranjan et al. demonstrated a physical interaction between DRP-1 and Rad50, a protein required in the initial steps of ATM-dependant dsDNA break repair (Guo et al. 2010; Ranjan et al. 2014).

In WT cells, dysfunctional mitochondrial fragments are repaired or removed from the mitochondria pool through various pathways including stress-induced

mitochondrial hyperfusion (SIMH) and mitochondrial autophagy. In SIMH, the damaged mitochondrial population favors a highly fused and polarized state, which is hypothesized to mitigate damage through mixing of mtDNA, proteins and lipids to buffer the damage (Shutt and McBride 2013). However, SIMH is considered a short term adaptive process, which can further contribute to mitochondrial damage as mixing of contents may spread detrimental components and prevent removal of the damaged mitochondrial fragments (Shutt and McBride 2013). When the damage reaches a critical threshold of both severity and time, mitochondria frequently undergo mitophagy, in which damaged mitochondrial fragments depolarize and are removed from the mitochondrial pool through DRP-1 dependant fission (Balaban et al. 2005; Frank et al. 2012). Our results suggest that the mutants have an impairment in this process, leading to dysfunctional mitochondrial units persisting in the cellular population, contributing to ROS production and consequential cellular damage.

We consistently observed that the p.T115M/T115M patient fibroblasts represented an intermediate phenotype between WT controls and the p.W88M*9/E129K*6 fibroblasts. An exception to this was mtDNA content, a surrogate for mitochondrial biomass, where the T115M/T115M cells had a larger magnitude of change compared to control. The p.W88M*9/E129K*6 fibroblasts had a lower oxidative capacity (OCR) and mitochondrial membrane potential and a higher level of ROS, all of which would normally lead to, or be indicative of, a lower mitochondrial mass in the cell. This inconsistency may represent a compensatory up-regulation of mtDNA, which has been observed in response to ROS stress (Lee and Wei 2005). Alternatively, previous investigation has shown that DRP-1 depleted cells have more damaged mtDNA (oxidative damage, less functional and transcriptionally active), with a disrupted distribution (large mitochondrial regions devoid of mtDNA and other areas with mtDNA clusters) (Parone et al. 2008). With reduced DRP-1 activity, mitophagy is impaired and damaged mitochondrial components remain in the cell, including oxidized mtDNA. Lacking this essential quality control process would likely result in accumulated mtDNA damage, contributing to decreased capacity and overall functional ability of the mitochondrial population in these mutants. In the case of the p.W88M*9/E129K*6 cells, quantity may not represent quality.

DRP-1 Plays a Role in Cellular Stress Response

In neurological disorders, oxidative stress and reactive oxygen species are both indicators of and causative factors in neuronal damage (Federico et al. 2012). As a result, ROS are kept under tight homeostatic control, with mitochondria being a producer and central regulator of ROS (Shadel and Horvath 2015). Loss of $\Delta\Psi_m$ is linked to oxidative stress, and can indicate initiation of mitophagy and mitochondria-dependant apoptotic pathways. This pattern was clearly observed in our WT control cells, with a dose-dependent reduction in $\Delta\Psi_m$ with peroxide exposure. However, both patient-derived samples showed a significantly blunted loss of $\Delta\Psi_m$ with oxidative stress (Fig. 7), indicating a maladaptive response, and potentially the induction of SIMH pathways as a last resort for cell survival (Shutt and McBride

2013). As mentioned above, DRP-1 also likely has a role in DNA repair, through interactions with Rad50 and p53. Our observation that both the p.T115M/T115M and p.W88M*9/E129K*6 cell lines had lower dsDNA repair responses to increasing oxidative stress is consistent with the idea that Rad50-dependant H2AX phosphorylation is a stress-dependant response. Other H2AX phosphorylating pathways may not be affected under basal conditions, resulting in the elevated γ-H2AX levels observed at baseline.

DNM1L Variant Influences Neurological Dysfunction

The cellular phenotype of the DRP-1 variants provides insight into how these mutations contribute to the clinical presentation of the patients. Consistent with previously described DRP-1 mutations, the disruption of mitochondrial fission leads to impaired mitochondrial spatial distribution within the cell, a change that is particularly important in neuronal function and during brain development. Mitochondrial derived energy and apoptotic signaling is essential for neurite formation and synaptic maintenance in fetal and post-natal CNS development (Ishihara et al. 2009; Wakabayashi et al. 2009). The combination of poor architecture with reduced gross mitochondrial amount and an impaired function of the remaining organelles means that the available cellular energy is reduced. The generation of action potentials and maintenance of the neuronal membrane potential normally requires up to 80% of the energetic reserve capacity of the cell, and a lower ATP availability dramatically reduces neuronal function and survival (Desler et al. 2012). Interestingly, developmental delays were not diagnosed until approximately a year of age in our patient, making it plausible that the p.T115M/T115M variant was compensated for until the post-infant developmental stage, or that the intermediate phenotype (compared to complete ablation of the protein or the more severe compound heterozygote we describe for comparison) was sufficient functionally until that time. In support for the latter, our findings that mitochondrial stress responses (in particular, the oxidative stress response) were profoundly affected by the p.T115M/T115M alteration indicates that the patient may have required some stress for the full impact of the mutation to be seen. This idea is consistent with the significantly elevated lactate levels observed in the patient during bacterial infection (but not at baseline). With an impaired stress response and elevated basal levels of ROS, our patient would likely experience progressive neural damage from dsDNA breaks, aggravating disease phenotype. The accumulation of DNA damage has been shown to contribute to the development of many neurological disorders such as ataxia telangiectasia, a disorder which shows many phenotypic similarities to our patient (Federico et al. 2012; Lavin 2008).

Acknowledgements The authors would like to acknowledge the Hospital for Sick Children David Fear Fund.

Funding This research did not receive any specific grant from funding agencies in the public, commercial, or not-for-profit sectors.

Compliance with Ethical Standards

Conflict of interest We have no conflicts of interest to report.

Ethical Statement All samples were collected after institutional ethics approval (Regional Ethics Board File Number: 1000009004) and approved parental consent. Each subject (parental caregivers) gave signed informed consent to sample acquisition, fibroblast isolation, analysis, and publication.

References

Adzhubei IA, Schmidt S, Peshkin L, Ramensky VE, Gerasimova A, Bork P et al (2010) A method and server for predicting damaging missense mutations. Nat Methods 7(4):248–249

Balaban RS, Nemoto S, Finkel T (2005) Mitochondria, oxidants, and aging. Cell 120(4):483–495

Benard G, Bellance N, James D, Parrone P, Fernandez H, Letellier T, Rossignol R (2007) Mitochondrial bioenergetics and structural network organization. J Cell Sci 120(5):838–848

Chang CR, Blackstone C (2010) Dynamic regulation of mitochondrial fission through modification of the dynamin-related protein Drp1. Ann N Y Acad Sci 1201(1):34–39

Chao Y-H, Robak LA, Xia F, Koenig MK, Adesina A, Bacino CA et al (2016) Missense variants in the middle domain of DNM1L in cases of infantile encephalopathy alter peroxisomes and mitochondria when assayed in Drosophila. Hum Mol Genet 25(9):1846–1856

Clinton RW, Francy CA, Ramachandran R, Qi X, Mears JA (2016) Dynamin-related protein 1 oligomerization in solution impairs functional interactions with membrane-anchored mitochondrial fission factor. J Biol Chem 291(1):478–492

Desler C, Hansen TL, Frederiksen JB, Marcker ML, Singh KK, Juel Rasmussen L (2012) Is there a link between mitochondrial reserve respiratory capacity and aging? J Aging Res 2012:192503

Dickey AS, Strack S (2011) PKA/AKAP1 and PP2A/Bβ2 regulate neuronal morphogenesis via Drp1 phosphorylation and mitochondrial bioenergetics. J Neurosci 31(44):15716–15726

Fahrner JA, Liu R, Perry MS, Klein J, Chan DC (2016) A novel de novo dominant negative mutation in DNM1L impairs mitochondrial fission and presents as childhood epileptic encephalopathy. Am J Med Genet A 170(8):2002–2011

Federico A, Cardaioli E, Da Pozzo P, Formichi P, Gallus GN, Radi E (2012) Mitochondria, oxidative stress and neurodegeneration. J Neurol Sci 322(1):254–262

Frank M, Duvezin-Caubet S, Koob S, Occhipinti A, Jagasia R, Petcherski A, Reichert AS (2012) Mitophagy is triggered by mild oxidative stress in a mitochondrial fission dependent manner. Biochim Biophys Acta Mol Cell Res 1823(12):2297–2310

Guo Z, Kozlov S, Lavin MF, Person MD, Paull TT (2010) ATM activation by oxidative stress. Science 330(6003):517–521

Guo X, Sesaki H, Qi X (2014) Drp1 stabilizes p53 on the mitochondria to trigger necrosis under oxidative stress conditions in vitro and in vivo. Biochem J 461(1):137–146

Hoppins S, Lackner L, Nunnari J (2007) The machines that divide and fuse mitochondria. Annu Rev Biochem 76:751–780

Ishihara N, Nomura M, Jofuku A, Kato H, Suzuki SO, Masuda K, Goto Y-I (2009) Mitochondrial fission factor Drp1 is essential for embryonic development and synapse formation in mice. Nat Cell Biol 11(8):958–966

Jendrach M, Mai S, Pohl S, Vöth M, Bereiter-Hahn J (2008) Short-and long-term alterations of mitochondrial morphology, dynamics and mtDNA after transient oxidative stress. Mitochondrion 8(4):293–304

Knott AB, Perkins G, Schwarzenbacher R, Bossy-Wetzel E (2008) Mitochondrial fragmentation in neurodegeneration. Nat Rev Neurosci 9(7):505–518

Koirala S, Guo Q, Kalia R, Bui HT, Eckert DM, Frost A, Shaw JM (2013) Interchangeable adaptors regulate mitochondrial dynamin assembly for membrane scission. Proc Natl Acad Sci 110(15):E1342–E1351

Lavin MF (2008) Ataxia-telangiectasia: from a rare disorder to a paradigm for cell signalling and cancer. Nat Rev Mol Cell Biol 9(10):759–769

Lee H-C, Wei Y-H (2005) Mitochondrial biogenesis and mitochondrial DNA maintenance of mammalian cells under oxidative stress. Int J Biochem Cell Biol 37(4):822–834
Manczak M, Sesaki H, Kageyama Y, Reddy PH (2012) Dynamin-related protein 1 heterozygote knockout mice do not have synaptic and mitochondrial deficiencies. Biochim Biophys Acta (BBA) 1822(6):862–874
Martelotto LG, Ng CK, De Filippo MR, Zhang Y, Piscuoglio S, Lim RS, Weigelt B (2014) Benchmarking mutation effect prediction algorithms using functionally validated cancer-related missense mutations. Genome Biol 15(10):484
Mears JA, Lackner LL, Fang S, Ingerman E, Nunnari J, Hinshaw JE (2011) Conformational changes in Dnm1 support a contractile mechanism for mitochondrial fission. Nat Struct Mol Biol 18(1):20–26
Nasca A, Legati A, Baruffini E, Nolli C, Moroni I, Ardissone A, Ghezzi D (2016) Biallelic mutations in DNM1L are associated with a slowly progressive infantile encephalopathy. Hum Mutat 37(9):898–903
Palmer CS, Osellame LD, Laine D, Koutsopoulos OS, Frazier AE, Ryan MT (2011) MiD49 and MiD51, new components of the mitochondrial fission machinery. EMBO Rep 12(6):565–573
Parone PA, Da Cruz S, Tondera D, Mattenberger Y, James DI, Maechler P, Martinou J-C (2008) Preventing mitochondrial fission impairs mitochondrial function and leads to loss of mitochondrial DNA. PLoS ONE 3(9):e3257
Qi X, Qvit N, Su Y-C, Mochly-Rosen D (2013) A novel Drp1 inhibitor diminishes aberrant mitochondrial fission and neurotoxicity. J Cell Sci 126(3):789–802
Ranjan R, Ahamad N, Ahmed S (2014) Fission yeast Drp1 is an essential protein required for recovery from DNA damage and chromosome segregation. DNA Repair 24:98–106
Reddy PH, Reddy TP, Manczak M, Calkins MJ, Shirendeb U, Mao P (2011) Dynamin-related protein 1 and mitochondrial fragmentation in neurodegenerative diseases. Brain Res Rev 67(1):103–118
Santos JH, Mandavilli BS, Van Houten B (2002) Measuring oxidative mtDNA damage and repair using quantitative PCR. Mitochondrial DNA Methods Protoc. https://doi.org/10.1385/1-59259-284-8:159
Schmid SL, Frolov VA (2011) Dynamin: functional design of a membrane fission catalyst. Annu Rev Cell Dev Biol 27:79–105
Schrader M (2006) Shared components of mitochondrial and peroxisomal division. Biochim Biophys Acta (BBA) Mol Cell Res 1763(5):531–541
Shadel GS, Horvath TL (2015) Mitochondrial ROS signaling in organismal homeostasis. Cell 163(3):560–569
Sheffer R, Douiev L, Edvardson S, Shaag A, Tamimi K, Soiferman D, Saada A (2016) Postnatal microcephaly and pain insensitivity due to a de novo heterozygous DNM1L mutation causing impaired mitochondrial fission and function. Am J Med Genet A 170(6):1603–1607
Shutt TE, McBride HM (2013) Staying cool in difficult times: mitochondrial dynamics, quality control and the stress response. Biochim Biophys Acta (BBA) Mol Cell Res 1833(2):417–424
Smirnova E, Griparic L, Shurland D-L, Van Der Bliek AM (2001) Dynamin-related protein Drp1 is required for mitochondrial division in mammalian cells. Mol Biol Cell 12(8):2245–2256
Strack S, Wilson TJ, Cribbs JT (2013) Cyclin-dependent kinases regulate splice-specific targeting of dynamin-related protein 1 to microtubules. J Cell Biol 201(7):1037–1051
Taguchi N, Ishihara N, Jofuku A, Oka T, Mihara K (2007) Mitotic phosphorylation of dynamin-related GTPase Drp1 participates in mitochondrial fission. J Biol Chem 282(15):11521–11529
Uo T, Dworzak J, Kinoshita C, Inman DM, Kinoshita Y, Horner PJ, Morrison RS (2009) Drp1 levels constitutively regulate mitochondrial dynamics and cell survival in cortical neurons. Exp Neurol 218(2):274–285
Vanstone JR, Smith AM, McBride S, Naas T, Holcik M, Antoun G et al (2015) DNM1L-related mitochondrial fission defect presenting as refractory epilepsy. Eur J Hum Genet 24:1084–1088
Wakabayashi J, Zhang Z, Wakabayashi N, Tamura Y, Fukaya M, Kensler TW, Sesaki H (2009) The dynamin-related GTPase Drp1 is required for embryonic and brain development in mice. J Cell Biol 186(6):805–816
Waterham HR, Koster J, van Roermund CW, Mooyer PA, Wanders RJ, Leonard JV (2007) A lethal defect of mitochondrial and peroxisomal fission. N Engl J Med 356(17):1736–1741
Westermann B (2010) Mitochondrial fusion and fission in cell life and death. Nat Rev Mol Cell Biol 11(12):872–884
Wilson TJ, Slupe AM, Strack S (2013) Cell signaling and mitochondrial dynamics: implications for neuronal function and neurodegenerative disease. Neurobiol Dis 51:13–26

Yoon Y, Pitts KR, Dahan S, McNiven MA (1998) A novel dynamin-like protein associates with cytoplasmic vesicles and tubules of the endoplasmic reticulum in mammalian cells. J Cell Biol 140(4):779–793

Yoon G, Malam Z, Paton T, Marshall CR, Hyatt E, Ivakine Z, Cohn RD (2016) Lethal disorder of mitochondrial fission caused by mutations in DNM1L. J Pediatr 171(313–316):e312

Zhao J, Liu T, Jin S, Wang X, Qu M, Uhlén P, Nistér M (2011) Human MIEF1 recruits Drp1 to mitochondrial outer membranes and promotes mitochondrial fusion rather than fission. EMBO J 30(14):2762–2778